JOURNAL OF MATERIALS SCIENCE 37 (2002) 655–662

High temperature bending creep of a Sm-α-β Sialon composite

MING-TONG LIN, LIN WANG, DAN-YU JIANG, GUO-QIANG ZHU, JIAN-LIN SHI*
The State Key Lab of High Performance Ceramics and Superfine Microstructure, Shanghai Institute of Ceramics, Chinese Academy of Sciences, Shanghai 200050, People's Republic of China
E-mail: jlshi@sunm.shcnc.ac.cn

The four-point bending creep behavior of a Sm-α-β Sialon composite, in which Sm-melilite solid solution (denoted as M′) was designed as intergranular phase, was investigated in the temperature range 1260–1350°C and stresses between 85 and 290 MPa. At temperatures less than 1300°C, the stress exponents were measured to be 1.2–1.5, and the creep activation energy was 708 kJ mol^{-1}, the dominant creep mechanism was identified as diffusion coupled with grain boundary sliding. At temperatures above 1300°C, the stress exponents were determined to be 2.3–2.4, and creep activation energy was 507 kJ mol $^{-1}$, the dominant creep mechanism was suggested to be diffusion cavity growth at sliding grain boundaries. Creep test at 1350°C for pre-oxidation sample showed a pure diffusion mechanism, because of a stress exponent of 1. N^{3-} diffusing along grain boundaries was believed to be the rate controlling mechanism for diffusion creep. The oxidation and $\alpha \rightarrow \beta$ Sialon phase transformation were analyzed and their effect on creep was evaluated.

1. Introduction

α Sialon and β Sialon, isostructural with α Si_3N_4 and β Si_3N_4 respectively, are two principal Sialon ceramics of practical value, because of their excellent mechanical properties and oxidation resistance. Usually, α Sialon has equiaxed grain morphology and higher hardness, β Sialon grains are acicular with aspect ratio >4 and have higher strength and toughness. Sialon ceramics with both higher hardness and higher strength can be achieved through designing α/β Sialon composites. Meanwhile, the combination between Sialon grains has a great influence upon mechanical properties of Sialon ceramics. Designing high refractory and high melting point intergranular phase is an effective way to improve the creep behavior of Sialon ceramics. At present, Sm-melilite solid solution (M′) is one of the most commonly used Sialon intergranular phases [1–7].

Creep rupture is the major damage form for Sialon ceramics being used at high temperature. Sialon ceramics are classified into two catalogs, one contains amorphous intergranular phase, the other contains crystalline intergranular phase. The steady state creep mechanisms of Sialon ceramics containing amorphous intergranular phase has been attributed to viscous flow, grain boundary sliding, diffusion and cavities. In contrast, diffusion is the primary mechanism for the creep of Sialon ceramics containing crystalline intergranular phase. A large number of creep data of Si_3N_4 ceramics prepared by various methods such as HP or HIP have shown their stress exponents within the range of 1 and 3 [8], and creep activation energy Q between 550–750 kJ mol^{-1} [8–10], by the mechanisms of diffusion, grain boundary sliding and cavity. Stress exponent is supposed to be greater than 3 for dislocation deformation. So far, very few dislocation phenomena have been observed by microstructure observation during the creep of Si_3N_4 ceramics, because only at temperature higher than 1400°C [11] can dislocation mechanisms be activated in Si_3N_4 ceramics.

Due to the different microstructure and composition, α and β Sialon have distinct contribution to creep resistance. Klemm *et al*. [12] pointed out that creep resistance was enhanced with the increase of α Sialon content in the study of four point bending creep of α/β Sialon composite using YAG as intergranular phase. They attributed the improved creep resistance to the thinner grain boundaries between α Sialon grains and a strong creep resistance skeleton. However, Wereszczak *et al*. [13] drew opposite conclusion, in the creep of Y_2O_3-doped Si_3N_4, that the creep behavior degraded as α Sialon content was increased. Schneider *et al*. [14] studied the influence of grain morphology of MgO/Y_2O_3 doped Si_3N_4 on creep behavior and discovered that n value is close to 2 for equiaxed α grain and 1 for acicular β grain.

Bending creep is still one of the most popular approaches to investigate the creep behaviour of ceramics at high temperature [15], because of its simplicity and economy. Much work has been done on the creep behavior of Sialon ceramics [16–22], however, hardly any

*Author to whom all correspondence should be addressed.

reports could be found in the literature on the creep of Sm-α-β Sialon composite. In this paper, the creep behavior of a Sm-α-β Sialon composite with an original α/β ratio of 55/45 is presented.

2. Experimental procedure

2.1. Materials

Sialon composite was prepared, using the powders of Si_3N_4 (UBE, SN-E10), Al_2O_3 (Shanghai Chemical Works), AlN (by our laboratory) and Sm_2O_3 (>99.9%, Shanghai Chemical Reagent Corporation) as the starting materials. The composition lies at the α and β Sialon coexisting area of Si_3N_4-4/3AlN:Al_2O_3-SmN:3AlN compatibility triangle within Janecke prism [1], as circled in Fig. 1 ($z = 0.8$ for β Sialon, $m = 1.0$ and $n = 1.5$ for α Sialon). The batch was well mixed in alcohol and milled in a plastic bottle for 48 hours using Sialon balls as milling media. After being dried, the powder was sieved and packed into a graphite die and sintered for 1 hour with a load of 24 MPa and temperature 1800°C in N_2 atmosphere, and disks of 70 mm in diameter were fabricated. Then the disks were cut into testing bars in dimension of $2 \times 4 \times 40$ mm^3, and the tensile surfaces were carefully polished with 0.5 μm diamond paste. Before creep test, the samples were heat treated at 1550°C for 6 hours in N_2 atmosphere, so that more α Sialon could be transformed to β Sialon.

The mechanical properties of the samples after heat treatment were listed in Table I. Vicker's hardness testing was conducted on AKASHI (AVK-A) hardness tester with an applied load of 10 kg for 10 seconds. The fracture toughness K_{IC} was determined by single-edge notched beam (SENB) method using $2.5 \times 5 \times 26$ mm^3 rectangle samples with a notch width of 0.2 mm and depth of 2.5 mm. The bending strength was measured in air in three-point geometry with a span of 30 mm for room temperature, using testing bars with dimensions of $3 \times 4 \times 36$ mm^3. Both fracture toughness and bending strength tests were performed on INSTRON 1195. The density measurements were carried out according to Archimedes' principle in distilled water.

TABLE I Physical properties of as heat-treated samples

H_{v10} GPa	K_{IC} MPa m$^{1/2}$	σ_b MPa	ρ/ρ_{th} %
17.2	5.3	747	99.2

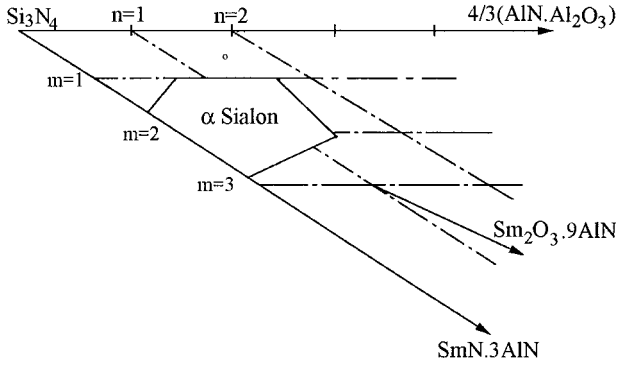

Figure 1 The sample composition in α Sialon plane.

2.2. Creep testing

Creep tests were conducted on four-point bending apparatus with a cantilever of 8:1, and the fixture was made of pure SiC with inner and outer span of 10 mm and 30 mm, respectively. The samples were heated in a furnace with a Pt-Rh element which offered ±2°C of temperature control. The center deflection of outer tensile fiber was accumulated by a linear variable differential transformer (LVDT) and recorded by a personal computer with an accuracy of ± 1 μm. The temperature increased at a rate of about 5°C per minute, and the system was held at given temperature for 0.5 hour before loading. All the tests were carried out in air.

2.3. Oxidation analysis

Oxidation of the samples during test was surveyed with SEM, including surface morphology and thickness of oxidation scale, and by weighing the samples before and after creep. The oxidation of Sialon was assumed to obey the parabolic law [1], by which the oxidation rate constants k were assessed, and apparent oxidation activation energy was attained by Arrhenius plots between k and $1/RT$.

2.4. Microstructure examination

The grain morphologies and intergranular phases of the samples before and after creep test were examined by transmission electron microscopy (TEM) and high resolution electron microscopy (HREM). The crept samples for TEM and HREM analysis were taken from the tensile sides of the specimens, and prepared by ion-beam thinning till suitable for TEM observation. A thin layer of carbon was deposited on the surface to minimize charging under the electron beam. Grain sizes of materials were calculated by an intercept method.

2.5. X-ray diffraction

One as-heat-treated sample and two crept samples were examined by XRD (RAX-10, Riagaku, Cu k_α). For crept samples, the oxidized layers were removed and the tests were conducted on the tensile sides. The contents of α Sialon, β Sialon and intergranular phase of the above samples were determined with a method similar to that used by Gazzara and Messier [23] based on the data of X-ray diffraction.

3. Results

3.1. Creep behavior

All the measured strain-time curves show primary and secondary creep, but no tertiary creep. Fig. 2 shows examples of strain-time curves. The time for primary creep is between 5–30 hours depending on the testing condition, samples crept at the higher temperature, could sustain for the longer transient state. Creep mechanism for primary creep, we believe, is grain boundary sliding. All the curves have a quasi steady state. The typical length of time for bend creep studies of Si_3N_4 based ceramics in the literature varies anywhere from 20 to over 150 hours. Because of test fixture geometry and experimental logistics, extended test periods are impractical. Like that done by Cinibulk *et al.* [24], all tests were terminated before 150 hours.

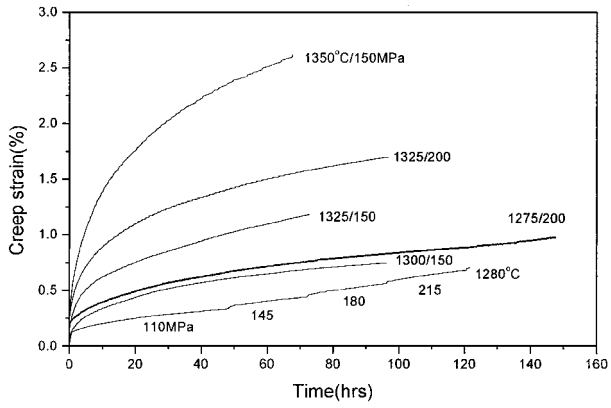

Figure 2 Bending creep curves.

3.2. Microstructure and X-ray diffraction

Microstructures consist of equiaxed α Sialon and elongated β Sialon and intergranular phases. No radical changes in microstructures of the samples have been observed during creep tests. Grain size of α Sialon is about 1 μm, the aspect ratio of β Sialon grains is around 5, and the thickness of intergranular phase is about 1 nm. Fig. 3a shows grain morphologies of specimens before creep tests. From the TEM results for crept samples in Fig. 3b–e, cavities at grain boundaries and in triple grain junctions could be found, and a few dislocations, which might be formed during sintering, were also detected in elongated β-Sialon grains. HREM observations (Fig. 4a and b) show that the disordered intergranular phases is

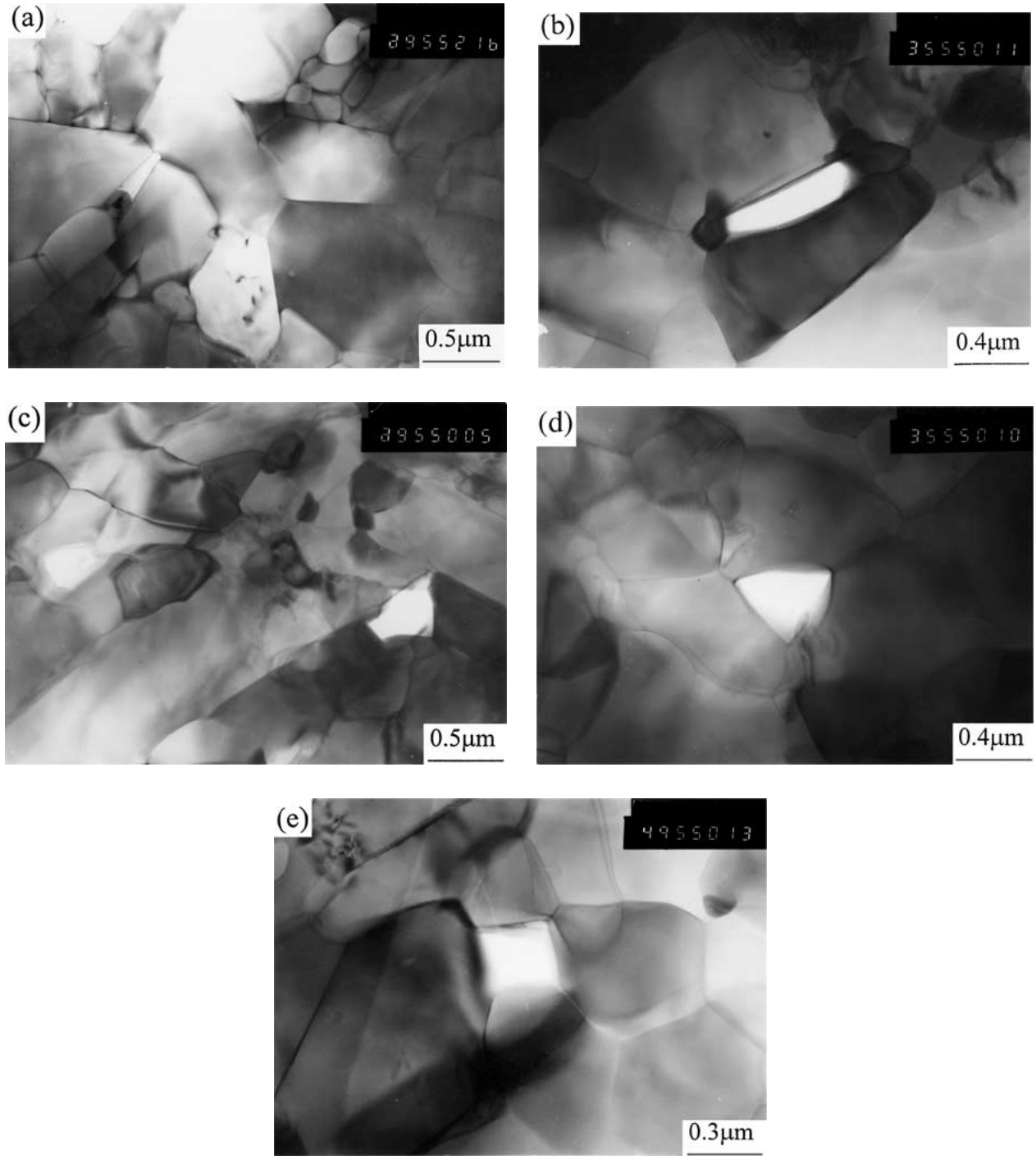

Figure 3 TEM micrographs of as-heat-treated and crept samples (a) as heat treated sample (b)–(e) crept for 148 hours at 1275°C and 200 MPa with a creep strain of 0.91%, showing intergranular and multi junction cavities.

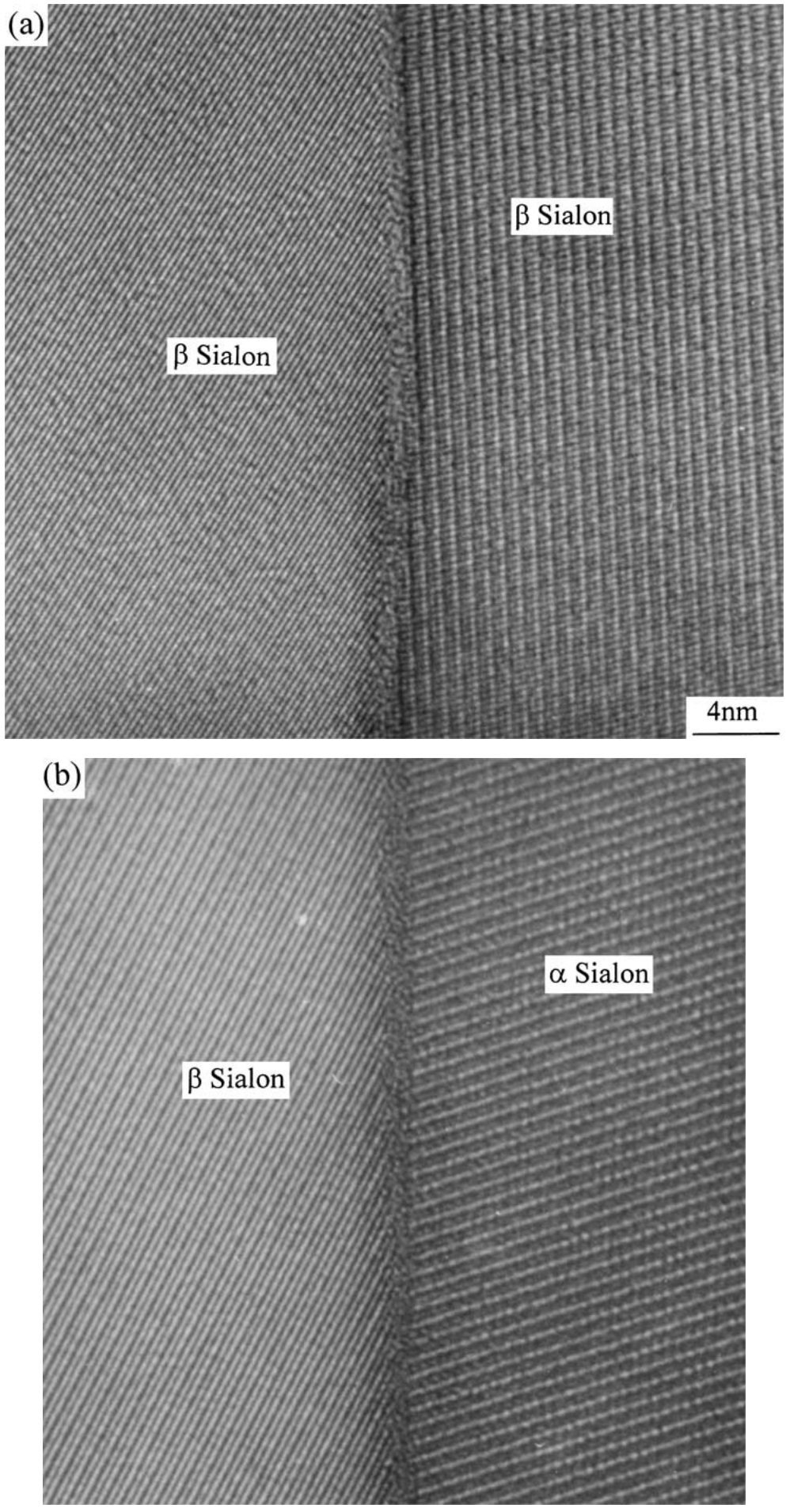

Figure 4 HREM micrographs of the sample crept for 67 hours at 1350°C and 150 MPa with a creep strain of 2.6%, showing α/β and β/β Sialon intergranular combination.

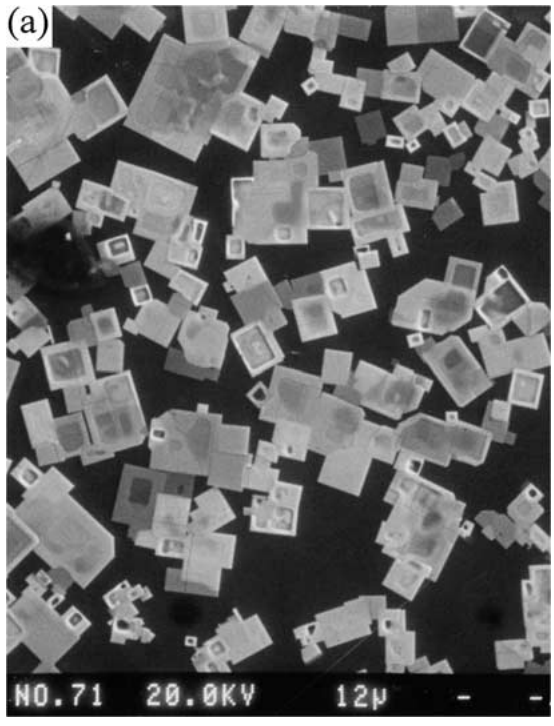

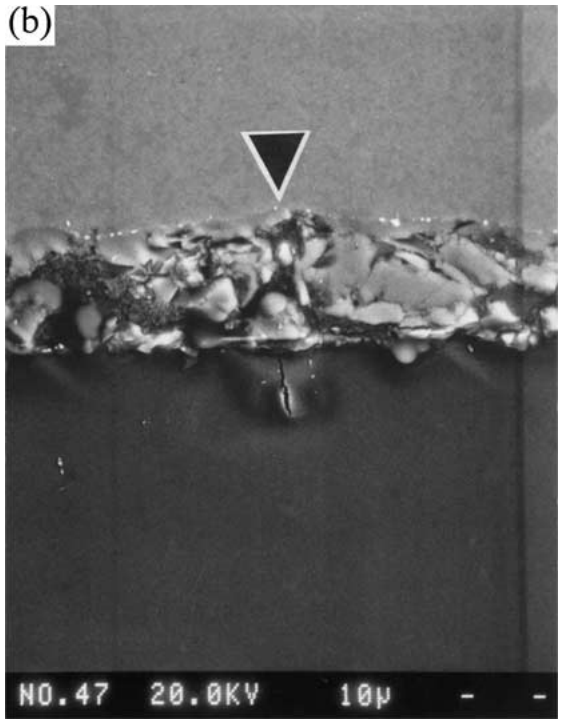

Figure 5 SEM micrographs of crept sample the same as that for Fig. 3b–e: (a) the morphology of oxidation surface (b) the thickness of oxidation scale.

very thin, and no obvious differences in thickness between α/β and β/β grain boundary could be found.

SEM results in Fig. 5a and b show the oxidation morphology and thickness of the oxidation scale. After creep, both tensile and compressive surface were covered with a film of glass in which the oxidation products $SmAlO_3$ (square), α-crystobalite, mullite and N_2 pores were embedded. The thickness of the oxidation scale varies with testing conditions, for the sample crept at 1275°C and 200 MPa for 148 hours, the oxidation scale is about 20 μm thick.

Fig. 6 shows the data of X-ray diffraction of samples before and after creep, which indicates that the ratio

TABLE II Phase ratio of α, β Sialon and Sm-melilite (M)

	$\beta/(\alpha+\beta)$	M/$(\alpha+\beta)$
A	45%	4.8%
B	61%	9.8%
C	39%	5.3%

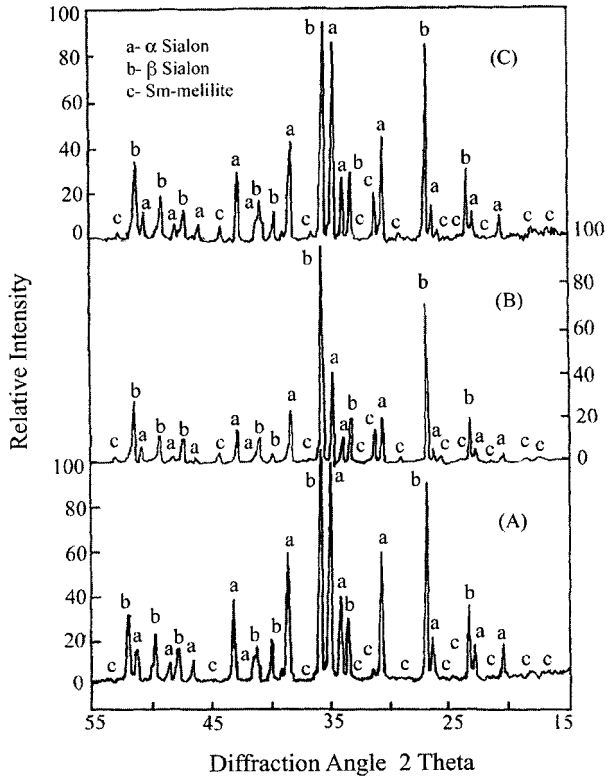

Figure 6 X-ray diffraction data of as-heat-treated and crept samples (A) as heat treated (B) the same sample as that for Fig. 4 (C) crept at 1300°C for 112 hours with a creep strain of 0.89%.

of α Sialon and β Sialon and content of intergranular phase changed due to the oxidation and the transformation from α Sialon to β Sialon, as listed in Table II. β Sialon grains and intergranular phases were consumed during oxidation and were also produced through the reconstruction of α Sialon to β Sialon during creep. The increase of M′ phase content during creep indicates that temperature is a determining factor for oxidation and phase transformation. For sample B, crept at 1350°C, more α Sialon had transformed to β Sialon than sample C crept at 1300°C. This is because at temperatures above eutectic point of Sm-Si-Al-O-N system (about 1300°C), a larger amount of liquid was formed which would greatly enhance the transformation of α Sialon to β Sialon.

3.3. Stress exponents, creep activation energies

The stress and temperature dependence of steady-state creep rate is usually expressed in following equation

$$\varepsilon_S = A\sigma^n \exp(-Q/RT) \quad (1)$$

Where ε_s is the steady-state creep rate, A is a preexponential factor depending on the material structure, σ is the applied stress, n is the stress exponent, Q is the creep activation energy, and RT has the usual meaning.

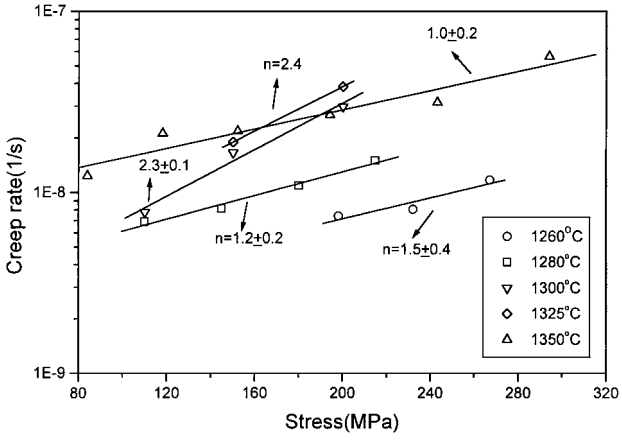

Figure 7 Steady state creep strain rate plotted against applied stress.

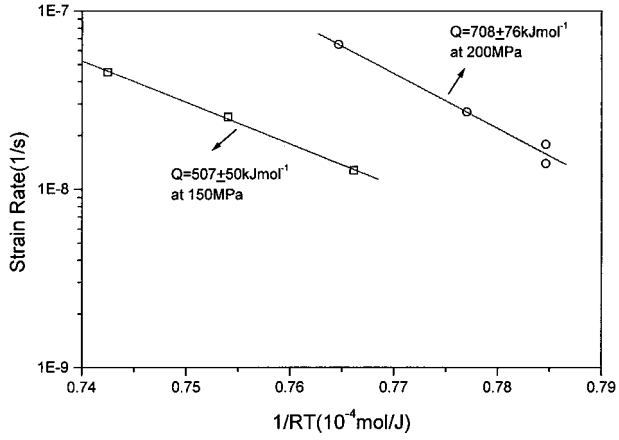

Figure 8 Arrhenius plots of steady creep rate.

By apparent linear fitting the data in Figs 7 and 8, we got the stress exponents n and creep activation energies Q at various conditions. In Fig. 7, the samples crept at 1300°C and 1325°C were tested by isothermal method, the others were tested by stress jump method. The samples crept at 1350°C was pre-oxidized at 1300°C for 51 hours. At temperature less than 1300°C, the stress exponents are 1.5 at 1260°C and 1.2 at 1280°C, which are close to those got by Xu *et al.* [11] for YL1, and by Cinibulk *et al.* [24] for $Sm_2Si_2O_7$-Si_3N_4 ceramics. At temperature higher than 1300°C, the stress exponents are 2.3 and 2.4 at 1300°C and 1325°C respectively, which are comparable to the values got by Todd and Xu [8] for Si_3N_4-$6Y_2O_3$-$2Al_2O_3$ and Xu *et al.* [11] for YL2. The creep activation energy, for the former, is 708 kJ mol^{-1}; and that, for the later, is 507 kJ mol^{-1}. The stress exponent for the pre-oxidized sample crept at 1350°C is 1.0, which approaches that got by Lange *et al.* [25] for pre-oxidized Si_3N_4/MgO alloys.

4. Discussions

4.1. Steady state creep mechanisms

Diffusion is assumed to be the major steady state creep mechanism for ceramics [26]. For Sialon ceramics, the diffusion species include Al^{3+}/O^{2-}, Si^{4+}/N^{3-} and additive cation Me^{v+}, two diffusion channels, bulk diffusion and grain boundary diffusion, are available for these species. Bulk diffusion occurs at higher temperature than grain boundary diffusion. Kijima and Shirasaki [27] gave the values of 238 kJ mol^{-1} and 778 kJ mol^{-1} through the measurement of the self diffusion coefficients for N^{3-} in single crystal grains of polycrystalline α and β Si_3N_4, respectively. Ziegler [28] found the value was 645 kJ mol^{-1} for N^{3-} diffusing via grain boundary phase in MgO-doped Si_3N_4.

The nucleation and growth of cavity are considered as the major damage form for Si_3N_4 ceramics crept at high temperature [29, 30]. Actually, the observed cavities, which are almost always located at two-grain boundaries and triple grain junctions, are denoted as R-type cavities and W-type cavities, respectively. TEM observations for crept samples show that most of the cavities are W-type cavities. This phenomenon indicates that grain boundary sliding plays an important role on the creep of the Sialon composite. No strain whorls, as reported by Crampon *et al.* [31] and Lange *et al.* [32], were observed by TEM on the tensile sides of crept samples. The reason is that, on the one hand, the test we conducted is bending creep, rather than compressive creep; on the other hand, Sialon grains are hard and the grain facets are smooth. Also, we can see that, from HREM observations, the grain boundary is very thin, only a very small amount of disordered phase exists on the grain boundary, so we can deduce that the grain boundary sliding is non-viscous. At $T < 1300$°C, i.e. the eutectic temperature of Sm-Si-Al-O-N system, the stress exponent is about 1.2–1.5 and creep activation energy is 706 kJ mol^{-1}, which suggests that the steady state creep mechanism is diffusion accommodated by grain boundary sliding. The diffusion is controlled by N^{3-} diffusing along grain boundaries [8, 16]. For this kind of coupled mechanism, Stevens [33] provided theoretical estimation for the contribution of grain boundary sliding to total creep strain. For model A

$$\Gamma_s = \frac{3[\exp(-\varepsilon_d) + \exp(\varepsilon_d)]}{4[4\exp(-\varepsilon_d) - \exp(\varepsilon_d)} \tag{2}$$

and for model B

$$\Gamma_s = \frac{4\exp(\varepsilon_d) - [4\exp(2\varepsilon_d) - 3]^{1/2}}{2[4\exp(2\varepsilon_d) - 3]^{1/2} + 4\exp(\varepsilon_d)} \tag{3}$$

where, Γ_s is the ratio of creep strain by sliding to the total strain, ε_d the strain by diffusion. In our experiment, all the total strains $\varepsilon_t < 3\%$, so $\Gamma_s \approx 0.5$ for both models.

For further consideration, Raj and Ashby [34] gave an expression of creep rate coupled with grain boundary sliding by assuming that all the grains are hexagonal and have periodical boundary condition, viz:

$$\varepsilon_s = C\frac{\pi\sigma\Omega}{kT}\frac{D\delta}{d^2\lambda} \tag{4}$$

where, ε_s is steady creep rate, λ is wavelength of the periodical grain boundaries, $C = 42$, and the rest parameters have the same meaning in Coble diffusion equation [35], when the lattice diffusion is neglected. For the sample crept at 1350°C/150 MPa, we get $\varepsilon_s = 3.67 \times 10^{-8}\,s^{-1}$ through creep test, taking $\Omega = 7 \times 10^{-29}\,m^3$, $\delta = 10^{-9}$ m, $d \approx \lambda = 1\,\mu$m, the self diffusion coefficient D in Equation 4 is 5.9×10^{-19} m^2/s, which

is about three orders higher than the self-diffusion data of 3.9×10^{-24} m^2/s and 6.0×10^{-23} m^2/s given by Kijima and Shirasaki [26] at the same temperature for the single crystal grains of polycrystalline α and β Si_3N_4, respectively. This result supports the idea that N^{3-} diffusing along the grain boundaries is the rate controlling mechanism for diffusion creep.

AT $T \geqq 1300°C$, the stress exponent is about 2.3 and creep activation energy is 507 kJ mol^{-1}. The liquid intergranular phase enhanced the solution-diffusion-precipitation of α and β Sialon grains. The creep mechanism is attributed to diffusion cavity growth at sliding grain boundary. Raj and Ghosh [36] related the ratio of creep rate by Coble diffusion to total creep rate by cavity, i.e.

$$\frac{\varepsilon_{\text{coble}}}{\varepsilon_{\text{cavity}}} = 1.19\left(\frac{a}{d}\right)^2\left(\frac{a}{2r}\right) \tag{5}$$

where, a is the space of the cavities, r radius of cavities, and d grain size, as defined in Hull-Rimmer model [37].

For the pre-oxidized sample, which was crept at 1350°C, the stress exponent of 1 in Equation 1 indicates that the steady state deformation mechanism is pure diffusion, because of the compositional change induced by oxidation.

4.2. Oxidation and $\alpha \rightarrow \beta$ Sialon phase transformation during creep

A large amount of work has been done on the oxidation of Sialon ceramics. Generally, Sialon oxidation complies with parabolic law [1, 38].

$$(w/A)^2 = kt \tag{6}$$

Where w is weight gain, A surface area of the specimen, k oxidation rate constant, and t time. The effect of stress on oxidation activation energy can be expressed as follow:

$$E_{a'} = E_a + \sigma V^* \tag{7}$$

Where $E_{a'}$ is apparent oxidation energy under stress σ, E_a is that when $\sigma = 0$, V^* is volume constant. In our experiment, $E_{a'}$ was estimated to be 800–1000 kJ mol^{-1}, higher than creep activation energies.

Because of the different surface condition of the samples, the existence of active centers causes local stress concentration and inhomogeneous oxidation scale, as shown in Fig. 5b. From this point, the oxidation is detrimental to creep resistance. Meanwhile, glassy phase formed during oxidation fills the cracks and cavities, and the sample surface is covered with a thin passive film, which alleviates the stress concentration and increases the creep resistance. Owing to no disastrous oxidation happens under testing temperatures, as reported by Bouarroudj *et al*. [39] under 1400°C in Y_2O_3 doped Sialon, oxidation is assumed to be favorable for creep resistance. Grain boundary phase becomes thinner [40] and the cohesion between grains becomes stronger, and creep rate decrease during oxidation, since intergranular phase was consumed by diffusing to surface to form glassy phase. The observation of HREM indicates that almost all intergranular phase is Sm-melilite after heat treatment. During oxidation, Si^{4+} , Al^{3+} , Sm^{3+} and N^{3-} diffuse outward, and O^{2-} diffuse inward through the oxidation scale. According to EDS (Energy Dispersive Spectroscopy) analysis of the oxidation scales in Fig. 5, the oxidation products are $SmAlO_3$, N_2, crystabolite, mullite and Sm-Si-Al-O glass. The following reactions have been suggested [6]:

$$Si_{5.2}Al_{0.8}O_{0.8}N_{7.2} + 10.8O_2 \rightarrow 5.2SiO_2 + 0.4Al_2O_3 + 3.6N_2 \tag{8}$$

$$Sm_{0.33}Si_{9.5}Al_{2.5}O_{1.5}N_{13.5} + 10.87O_2 \rightarrow 0.33SmAlO_3 + 8.78SiO_2 + 0.36Al_6Si_2O_{13} + 6.75N_2 \tag{9}$$

Wilkinson [38] outlined the diffusion model for Me-α-β Sialon composite. Oxidation occurs at the surface scale by nitrogen and oxygen exchanging their charges. N^{3-} transporting from the bulk to the surface through the intergranular phase is more difficult than O_2 through oxidation scale, because the oxidation scale is glassy and the intergranular phase is almost crystalline. So, N^{3-} diffusion is the rate controlling oxidation mechanism. Nevertheless, at the experimental temperatures, the glassy oxidation scale can not be formed without the solvent Sm^{3+}, which has the same diffusion path as N^{3-}. The diffusion of Sm^{3+} plays an important role on oxidation, Mieskowski *et al*. [41] assumed it as the controlling mechanism for oxidation.

Two reasons contribute to $\alpha \rightarrow \beta$ Sialon phase transformation. One is the unparalleled oxidation of α and β Sialon grains, the other is stress induced phase transformation. $\alpha \rightarrow \beta$ Sialon transformation can take place with or without liquid, i.e. [7]

$$\alpha + \text{L} \rightarrow \beta + \text{Sm-melilite} \tag{10}$$

or

$$\alpha \rightarrow \beta + \text{Sm-melilite} \tag{11}$$

$\alpha \rightarrow \beta$ transformation leads to the increase of intergranular phase Sm-melilite which is deleterious to creep resistance and the increase of β Sialon content which is assumed to be beneficial to creep resistance, as we can see from Table II, when temperature was higher than eutectic temperature of Sm-Si-Al-O-N system, remarkable $\alpha \rightarrow \beta$ transformation took place. Because intergranular phase content is a determining factor for creep resistance of Sialon ceramics, $\alpha \rightarrow \beta$ transformation degrades the creep performance of the α/β Sialon composite. From Fig. 5 and Table II, we can see the contents of the intergranular phase in both crept samples increase.

5. Summary

The four-point bending creep behavior for a Sm-α-β Sialon composite was investigated at temperatures between 1260–1350°C and stresses within 85–290 MPa, and the results are:

1. At temperature below 1300°C, the stress exponent n and creep activation energy Q are about 1.2–1.5 and 708 kJ mol^{-1}, respectively; at temperature above

1300°C, $n = 2.3$–2.4 and $Q = 507$ kJ mol^{-1}. The discrepancy of stress exponent and creep activation energy between the two temperature ranges is related to the eutectic point of Sialon intergranular phase at around 1300°C.

2. The steady state creep mechanisms are the diffusion accommodated by grain boundary sliding and grain boundary sliding accompanied by diffusion cavity formation at temperature lower and higher than 1300°C, respectively. N^{3-} diffusing along the grain boundaries is the rate controlling mechanism for diffusion creep.

3. Remarkable oxidation occurred during creep. Sialon oxidation has the same rate controlling mechanism as that for diffusion creep. Sialon oxidation improves the creep resistance of the Sialon composite.

4. At temperature 1350°C, pre-oxidation of the sample shifts the creep mechanism from cavity creep to pure diffusion creep.

5. $\alpha \rightarrow \beta$ Sialon transformation increases the content of the intergranular phase Sm-melilite and degrades the creep resistance, especially at temperature above the eutectic point of the intergranular phase.

Acknowledgements

This work was supported by the National Natural Science Foundation of China under grant 59772008. The authors are grateful to Drs. J. B. Ho and M. L. Ruan for TEM and HREM observations and Mrs. J. H. Gao for SEM observations.

References

1. Z. K. HUANG, S. Y. LIU, A. ROSENFLANZ and I. W. CHEN, *J. Amer. Ceram. Soc.* **79** (1996) 2081.
2. Z. K. HUANG and I. W. CHEN, *ibid.* **79** (1996) 2091.
3. M. MENON and I. W. CHEN, *ibid.* **78** (1995) 545.
4. Y. B. CHENG and D. P. THOMPSON, *J. Europ. Cerac. Soc.* **14** (1994) 13.
5. *Idem.*, *J. Amer. Ceram. Soc.* **77** (1994) 143.
6. L.-O. NORDBERG, M. NYGREN, P.-O. KALL and Z. SHEN, *ibid.* **81** (1998) 1461.
7. T. EKSTROM, L. K. L. FALK and Z. SHEN, *ibid.* **80** (1997) 301.
8. J. A. TODD and Z. Y. XU, *J. Mater. Sci.* **24** (1989) 4443.
9. M. K. FERBER and M. G. JENKINS, *J. Amer. Ceram. Soc.* **75** (1992) 2453.
10. R. RAJ and P. E. D. MORGAN, *ibid.* **64** (1981) C143.
11. Y. R. XU, X. R. FU and T. S. YAN, *Physica* B **150** (1988) 276.
12. H. KLEMM, M. HERRMANN, T. REICH, C. SCHUBERT, L. FRASSEK, G. WOTTING, E. GUJEL and G. NIETFELD, *J. Amer. Ceram. Soc.* **81** (1998) 1141.
13. A. A. WERESZCZAK and T. P. KIRKLAND, *J. Mater. Sci.* **33** (1998) 2053.
14. J. A. SCHNEIDER and A. K. MUKHERJEE, *J. Amer. Ceram. Soc.* **82** (1999) 761.
15. M. G. JENKINS, S. M. WIEDERHORN and R. K. SHIFER, in "Mechanical Testing Methodology for Ceramic Design and Reliability," edited by D. C. Cranmer and D. W. Richerson (Marcel Dekker, 1998) p. 171.
16. G. BERNARD-GRANGER, J. CRAMPON R. DUCOLS and B. CALES, *J. Europ.Ceram. Soc.* **17** (1997) 1647.
17. B. S. B. KARUNARATNE and M. H. LEWIS, *J. Mater. Sci.* **15** (1980) 449.
18. C. F. CHEN and T. Z. CHUANG, *Ceram. Eng. Sci. Proc.* **8** (1987) 796.
19. T. SHIOGAI, K. TSUKAMOTO and N. SASHIDA, *J. Mater. Sci.* **33** (1998) 769.
20. F. F. LANGE, B. I. DAVIS and D. R. CLARKE, *ibid.* **15** (1980) 601.
21. J. L. DING, K. C. LIU, K. L. MORE and C. R. BRINKMAN, *J. Amer. Ceram. Soc.* **77** (1994) 867.
22. S. M. WIEDERHORN, B. J. HOCHEY, D. C. CRANMER and R. YECKLEY, *J. Mater. Sci.* **28** (1993) 445.
23. C. P. GAZZARA and D. R. MESSIER, *Ceram. Bull.* **56** (1977) 777.
24. M. K. CINIBULK, G. THOMAS and S. M. JOHNSON, *J. Amer. Ceram. Soc.* **75** (1992) 2050.
25. F. F. LANGE, B. I. DAVIS and D. R. CLARKE, *J. Mater. Sci.* **15** (1980) 616.
26. A. H. CHOKSHI and T. G. LANGDON, *Mater. Sci. and Tech.* **7** (1991) 577.
27. K. KIJIMA and S. SHIRASAKI, *J. Chem. Phys.* **65** (1976) 2668.
28. G. ZIEGLER, J. HEINRECH and G. WOTTING, *J. Mater. Sci.* **22** (1987) 3041.
29. D. S. WILKINSON, in "Tailoring of Mechanisms Properties of Si_3N_4 Ceramics," edited by M. J. Hoffmann and G. Petzow (Kluwer Academic Publishers, Dordrecht/Boston/London, 1994) p. 327.
30. S. M. WIEDERHORN, W. E. LUECKE, B. J. HOCKEY and G. G. LONG, *ibid.* p. 305.
31. J. CRAMPON, R. DUCLOS and N. RAKOTOHARISOA, *J. Mater. Sci.* **28** (1993) 909.
32. F. F. LANGE, D. R. CLARKE and B. I. DAVIS, *ibid.* **15** (1980) 611.
33. R. N. STEVENS, *Phil. Mag.* **23** (1971) 265.
34. R. RAJ and M. F. ASHBY, *Met. Trans.* **2** (1971) 1113.
35. R. L. COBLE, *J. Appl. Phys.* **34** (1963) 1679.
36. R. RAJ and A. K. GHOSH, *Met. Trans.* **12A** (1981) 1291.
37. D. HULL and D. E. RIMMER, *Phil. Mag.* **4** (1959) 673.
38. D. S. WILKINSON, *J. Amer. Ceram. Soc.* **81** (1998) 275.
39. J. BOUARROUDJ, P. GOURSAT and J. L. BESSEN, *J. Mater. Sci.* **20** (1985) 1150.
40. M. K. CINIBULK and H. J. CLEEBE, *ibid.* **28** (1993) 5775.
41. D. M. MIESKOWSKI and W. A. SANDERS, *J. Amer. Ceram. Soc.* **68** (1985) C-160.

Received 25 April 2000
and accepted 2 October 2001